Exp Fluids (2011) 50:419–428
DOI 10.1007/s00348-010-0938-5

RESEARCH ARTICLE

Electrically rotating suspended films of polar liquids

R. Shirsavar · A. Amjadi · A. Tonddast-Navaei · M. R. Ejtehadi

Received: 2 March 2010 / Revised: 1 July 2010 / Accepted: 7 July 2010 / Published online: 4 August 2010

Abstract Controlled rotation of a suspended soap water film, simply generated by applying an electric field, has been reported recently. The film rotates when the applied electric field exceeds a certain threshold. In this study, we investigate the phenomenon in films made of a number of other liquids with various physical and chemical properties. Our measurements show that the intrinsic electrical dipole moments of the liquid molecules seems to be vital for the corresponding film rotation. All the investigated rotating liquids have a molecular electric dipole moment of above 1 Debye, while weakly polar liquids do not rotate. However, the liquids investigated here cover a wide range of physical parameters (e.g. viscosity, density, conductivity, etc.). So far, no significant correlation has been observed between the electric field thresholds and macroscopic properties of the liquids.

1 Introduction

Suspended liquid films as thin as hundreds of nanometers or less allow us to study physical phenomena in a quasi non-directional (2D) medium (Couder et al. 1989; Chomaz and Cathalau 1990; Rivera and Wu 2000; Huang et al. 2004). Hydrodynamical effects of applying electric field have been studied widely for the bulk of both in polar and non-polar liquids (Saville 1997; Green et al. 2000), but the electro-hydrodynamical (EHD) flow on the suspended films of liquids has been studied just for liquid crystals (de Gennes and Prost 1995; Chandrasekhar 1992). For example, applying sufficiently large electric fields can produce patterns of convective vortices in freely suspended films of some thermotropic liquid crystals in nematic (Faetti et al. 1983a, b), smectic (Morris et al. 1990; Daya et al. 1997) and also isotropic (Faetti et al. 1983a; Sonin 1998) phases.

Recently, it has been shown that EHD effects in suspended films of soap water can induce a rotation with a full control on the velocity and chirality (Amjadi et al. 2009). The device, called a *film motor*, consists of a liquid film on a two-dimensional frame connected to an electrolysis potential difference and laid in an external in-plane electric field which crosses the internal electrolysis current (Fig. 1a). When either the external field or the electrolysis voltage exceeds a certain threshold, while the other one does not vanish, the liquid film begins to rotate. The effect may have wide applications e.g. in mixing, both in micro- and nano-mechanical devices.

Some charge-based mechanisms may be suggested for explaining the film rotation, e.g. non-uniform ion distribution, caused by the external electric field (the electrophoresis effect) (Shiryaeva et al. 2009), ion jets in the electrolysis double-layers close to the electrodes (Chiragwandi et al. 2005), and the electric field interactions with surface charges induced on the fluid–air interfaces (Faetti et al. 1983a; Morris et al. 1990; Daya et al. 1997). However, there is enough evidence to show that none of these mechanisms are the dominant reasons behind the film rotation phenomenon (Amjadi et al. 2009).

In this paper, the viability of rotation in film motors involving liquids other than soap water is studied. Measurements applied to 39 liquids capable of producing stable suspended film, yet covering a wide range of physical and chemical properties, are presented. Our results indicate that only liquids with electrically polar molecules can rotate.

R. Shirsavar · A. Amjadi · M. R. Ejtehadi (✉)
Department of Physics, Sharif University of Technology, P.O. Box 11365-9161, Tehran, Iran
e-mail: ejtehadi@sharif.edu

A. Tonddast-Navaei
Birmingham, UK

Fig. 1 The set up of the experiment

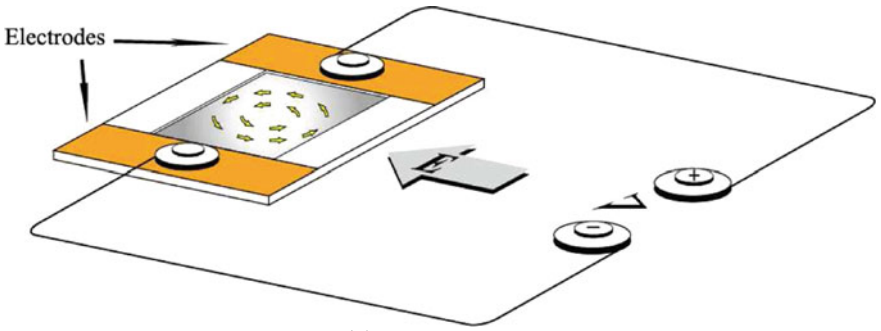

(a) The 3D sketch of the set up.

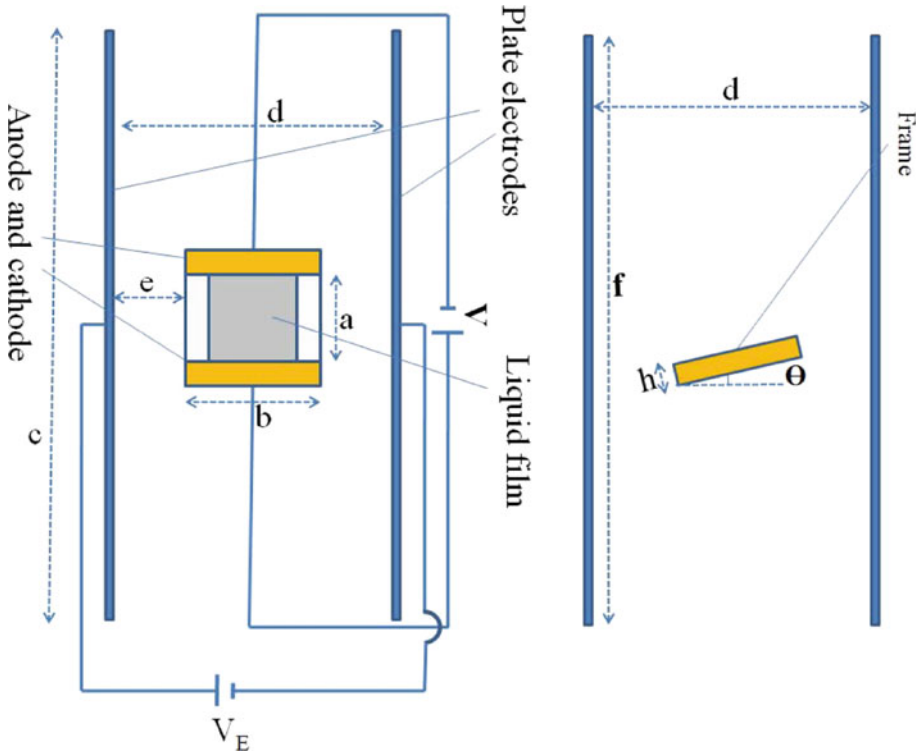

(b) Top view(left) and side view(right) of the set up of the experiment. In our set up all distances and lengths are changeable. Typical values are a=4mm, b=6mm, c=f=25mm, d=12mm, e=3mm, h=1mm and $\theta = 5^{\circ}$.

2 Instrumentation

2.1 Experimental setup

The main part of the experimental setup is an insulating frame with two graphite strips on two opposite sides of it, acting as electrodes (Fig. 1a). Frames of two different geometries, a 4 mm × 4 mm square and a 7 mm diameter circle, were used in this study; however, any other geometries could be incorporated. The freely suspended liquid film on the frame was created by brushing the liquid on it, where in this way, the liquid also dampened all the frame as well as the graphite electrodes. Connecting the electrodes to an electrolysis voltage V_{el} causes an average density of electric current $\mathbf{J}_{el}$ through the film. The frame was then located between two plates of a large capacitor with dimensions of 2.5 × 2.5 cm^2 and separation 12 mm, which produces an external electric field $\mathbf{E}_{ext}$ nearly in the plane of the film and almost perpendicular to the mean current density.

In all measurements, the frame dimensions were fixed to a small size of 4 × 4 mm^2, increasing the lifetime of the films. In order to avoid the effect of air flow on the liquid film, the setup was located inside a chamber. While the chamber helps with the undesirable effect of air flow, it does not prevent the physical and/or chemical interactions between air and the liquid molecules.

Two main factors cause liquid film thickness to change spatially and temporally: continuous evaporation of the film and the effect of gravitational force which induces the liquid flow to be biased toward the lower parts of the film. One may ride on the latter effect by slightly tilting the

frame horizontally which provides control over the liquid flow generated by gravity. A tilting angle of about 5° was found to create near-homogeneous color patterns such as Fig. 2a. The resulting color pattern is due to interference of light reflecting from the outer and inner surfaces of the film, which depends on the film thickness.

When the film frame is hold horizontally, the effect of gravity causes spatial and temporal changes in the thickness of the film, leading to an associated color pattern. This provides a simple way of visualizing the film thickness. It is known that any two adjacent constructive interference fringes have a half-wavelength difference in film thickness (Isenberg 1992). To have accurate thickness of the film, we need to know the order of interference for a mono color light. In the case of white light, the observed pattern of interference of films thicker than 1 μm is only composed of pink and green colors (Isenberg 1992; Rutgers et al. 2001).

Before each experiment, enough time was given to a freshly created film sloped a little (about 5°), until a small yellow region was observed on the top edge of the frame, being the thinner part of the film, from a point of view normal to the frame plane (Fig. 2a). This is a sign of forth-order interference, suggesting a film thickness between 600 and 800 nm (Isenberg 1992). Of course, this estimation depends on the liquid refractive index. As this quantity does not vary significantly for the selected liquids of this study, it does not affect the discussed rough estimation of film thickness. Using this approach, it was possible to achieve the same average film thickness at the threshold of rotation when performing different measurements.

For each given liquid, after setting the electric voltage on the graphite electrodes to the constant value of $V_{el} = 25$ V, the electric current passing through the film, I, was measured. Then an external electric field, $\mathbf{E}_{ext}$, nearly perpendicular to the electric current, was introduced where the electric field magnitude was increasingly changed from zero to a threshold causing the film to start rotating (Fig. 2b). At this point, the external electric field threshold,

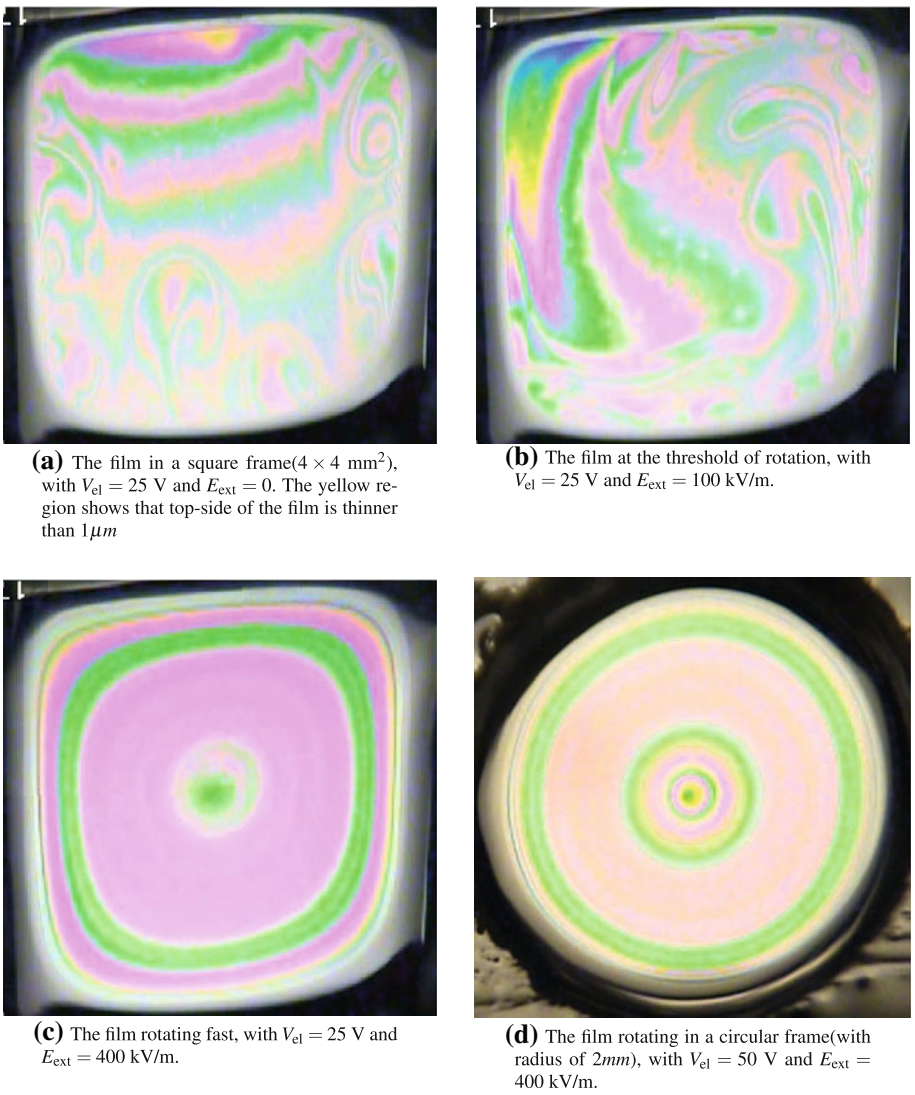

(a) The film in a square frame(4×4 mm^2), with $V_{el} = 25$ V and $E_{ext} = 0$. The yellow region shows that top-side of the film is thinner than $1\mu m$

(b) The film at the threshold of rotation, with $V_{el} = 25$ V and $E_{ext} = 100$ kV/m.

(c) The film rotating fast, with $V_{el} = 25$ V and $E_{ext} = 400$ kV/m.

(d) The film rotating in a circular frame(with radius of $2mm$), with $V_{el} = 50$ V and $E_{ext} = 400$ kV/m.

Fig. 2 Some film of Methyl 2-pyridyl ketone with different electrode voltage, external electric field values and frames. All films are nearly horizontal

Table 1 Some liquids with unstable films

Acetone	Acetonitrile
Cyclohexylamin	Ethanol
Ethanolamine	Heptane
Hexane	Methanol
Trimethylphosphate	Tetrachloroethylene
Carbontetrachloride	Toluene

E_T, and the corresponding current were recorded. This procedure was repeated a few times for each liquid resulting with an average value for E_T and I.

2.2 Material

Unlike soap water, the majority of liquids are not able to produce stable films. For instance, highly volatile liquids, such as acetone and methanol, evaporate very fast at room temperature leading to short-life films. Some liquids with unstable films, which were avoided in our measurements, are listed in Table 1.

As given in Tables 2 and 3, 39 liquids (Merk & Co Inc., NJ USA), known to make stable films, were picked for the experiments. All liquids had a purity of over 95% and were used without any additions or solvents. Since viscosities of some of the liquids were not provided by the vendor, a Physica MCR-301 rheometer (Anton Paar, Austria) was applied to address this.

2.3 Data acquisition

Color images of rotating films under study were captured using a Sony DCR-DVD705 camera. For each measurement, a set of consecutive images with the exposure time of 0.01 ms were generated, where the time separation between each frame was 40 ms.[1]

Due to the spatial gradient of film thickness, the recorded images of rotating films involved a strong color pattern. This pattern eliminated the need for using tracer particles as visualizers for extracting the velocity field.

2.4 Data analysis

2.4.1 Particle-image velocimetry

Particle-Image Velocimetry (PIV) is a well-established analysis technique in fluid mechanics which can extract the fluid flow velocity field at many points simultaneously (Adrian et al. 1991; Westerweel 1993). The analysis input usually includes two successive images of visualized fluid flow, with a short-enough time separation. This 'double-frame' is then divided into local small regions, and the pixel values of each corresponding regions in the double-frame are correlated to each other, resulting a displacement vector representing those regions. Repeating this on all of the local regions yields the displacement field.

When the flow of interest is in (quasi-)steady state, as in the case of this work, one can take advantage of the contribution of many double-frames in order to effectively increase the velocity field estimation accuracy. In correlation-based PIV analysis, this method is better known as ensemble correlation (Deen et al. 1999).

2.4.2 Variational image velocimetry

One of the main limitations of the traditional correlation-based PIV approach is the trade-off between velocity field spatial resolution and its accuracy. As a result, achieving single-pixel resolution by the correlation-based approach, if not impossible, is difficult. When applied to film motors, the single-pixel accuracy feature can be a valuable tool in studies such as accurate estimation of angular velocity about the rotation center. Another source of the error in the reported values is the statistical dispersity of the data due to difficulties in reproducing films with the same thickness profile.

Attempts have been made to apply the variational optic flow (Horn and Schunck 1981), a method mainly developed in the computer vision domain, to fluid flow estimation (Ruhnau et al. 2005). This approach tries to find the displacement field, registering the successive images, as a numerical solution of a variational optimization problem. The discussed resolution-accuracy compromise is not applied to variational-based PIV analysis, which makes it a preferable choice in the context of this work.

In analogy to ensemble correlation, more than one double-frame may be involved to improve the estimation of variational image velocimetry. Detailing the variational ensemble image velocimetry method is beyond the scope of this paper, and we simply present the analysis results produced by this technique.

3 Results

Our measurements show that when a sufficiently strong electric field is applied to the film, in the presence of an electric potential difference between the two electrodes, the liquids may be categorized into two groups:

Rotational liquids Given a certain external electric field threshold, films made of these liquids eventually start rotating (Fig. 2c, d). Examples are Anisole and Diethyl Oxalate.

Non-rotational liquids Regardless of how strong the external electric field is, films made of these liquids

[1] Movies are available from http://softmatter.cscm.ir/FilmMoto.

Table 2 Rotational liquids

Name	M (g/mol)[b]	μ (Debye)	ρ (g/cm^3)[b]	ε[c]	η (mPa.s)[c]	Critical force	I (μA)	E_T (kv/m)
1,2-Dichlorobenzene	147	2.5[c]	1.3	10.12	1.32[c]	1.34	0.11 ± 0.03	71 ± 9
1,3-Dichlorobenzene	147	1.72[c]	1.28	5.02	1.04[c]	0.85	<0.01	83 ± 7
1-Bromo-2-fluorobenzene	175	2.43[c]	1.6	4.72	1.14[f]	0.8	0.06 ± 0.02	95 ± 8
1-Bromo-3-fluorobenzene	175	1.55[c]	1.56	4.85	0.92[f]	0.54	0.05 ± 0.02	103 ± 9
4-Benzylpyridine	169.22	2.87[d]	1.06	–	4.70[f]	20.84	0.02 ± 0.01	110 ± 17
Aniline[a]	93.13	1.13[c]	1.02	7.06	3.85[c]	14.53	0.1 ± 0.02	80 ± 14
Anisole	108.13	1.38[c]	0.99	4.30	1.05[c]	1.11	<0.01	51 ± 8
Benzonitrile	103.12	4.18[c]	1.01	25.9	1.26[c]	1.57	0.75 ± 0.25	96 ± 8
Benzyl chloride	126.58	1.82[c]	1.53	6.854	1.28[c]	1.07	0.15 ± 0.5	76 ± 11
Chlordiphenyl methan	202.68	2.43[d]	1.14	–	6.30[f]	34.82	0.03 ± 0.01	125 ± 15
Ethyl benzoate	150.17	2.00[c]	1.05	6.02	1.70[f]	2.75	<0.01	64 ± 7
Methyl 2-pyridyl ketone	121.13	4.85[d]	1.08	–	1.70[f]	2.68	2.0 ± 0.5	92 ± 12
Methyl 3-pyridyl ketone	121.13	4.21[d]	1.1	–	2.90[f]	7.65	80 ± 15	99 ± 10
Methyl 4-pyridyl ketone	121.13	2.34[d]	1.09	–	2.30[f]	4.85	0.48 ± 0.08	69 ± 4
N,N-dimethylaniline	121.18	1.68[c]	0.95	4.90	1.3[c]	1.78	<0.01	89 ± 4
O-toluidine[a]	107.1	1.6[c]	1	6.138	3.82[c]	14.59	0.03 ± 0.01	122 ± 17
Pyridine	79.1	2.21[c]	0.98	13.260	0.87[c]	0.77	3.0 ± 0.5	79 ± 8
1−Butanol[a]	74.12	1.66[c]	0.81	17.84	2.54[c]	7.96	0.73 ± 0.15	107 ± 22
1−Methyl 2−pyrrolidone	99.13	4.1[c]	1.03	32.55	1.56[f]	2.36	15 ± 4	167 ± 15
1−Octanal	130.23	1.76[c]	0.82	10.30	7.28[g]	64.63	<0.01	87 ± 10
2,5−Hexanedione	114.14	1.46[d]	0.97	–	1.60[f]	2.64	1.0 ± 0.2	104 ± 18
Acetic acid[a]	60.05	1.7[c]	1.04	6.20	1.05[c]	1.06	9 ± 2	68 ± 3
Diethyl oxalate	146.1	2.49[c]	1.07	8.266	1.60[f]	2.39	0.5 ± 0.1	119 ± 14
Diiodomethane	267.83	1.08[c]	3.32	5.32	2.78[e,f]	2.33	<0.01	228 ± 16
Dimethyl sulfoxide	78.1	3.96[c]	1.1	47.24	1.99[c]	3.60	8.5 ± 1.5	90 ± 15
Ethylene glycol[a]	62.6	2.36[c]	1.11	41.4	16.1[c]	233.52	1.2 ± 0.2	106 ± 7
N,N−dimethylformamide	73.09	3.82[c]	0.94	38.25	0.79[c]	0.66	15 ± 3	60 ± 10
Piperidine[a]	85.15	1.19[c]	0.862	4.33	1.57[c]	2.86	0.25 ± 0.07	126 ± 18

Liquids are classified in two groups, Aromatic (bold) and non-Aromatic (italic)

[a] Protic liquid which contains dissociable H^+

[b] The Merck Chemicals Databases, http://www.merck-chemicals.com

[c] CRC Handbook of Chemistry and Physics, David R. Lide, ed., Internet Version 2005, http://www.hbcpnetbase.com, (CRC Press, Boca Raton, FL, 2005)

[d] Calculated by Gaussian98. The calculation error is about 20%

[e] Measured at shear rate of 10 s^{-1} (non-Newtonian fluid)

[f] Measured by a rotational rheometer as described in Sect. 2.2. The measurement error is about 10%

[g] Databook on the Viscosity of Liquids, D. S. Veswanath and G. Natarajan (Hemisphere, New York, 1989)

never start rotation. Examples are Mesitylene and n-Dodecane.

Out of the 39 investigated liquids, 28 were found to be rotational (Table 2) where 11 showed the non-rotational liquid traits (Table 3).

3.1 Rotational liquid characteristics

Direction and velocity of the film can be controlled via both external electric field and electrodes voltage difference: By keeping one of these two quantities constant, sign and magnitude of the other quantity determines film rotation direction and velocity field magnitude at a given position on the film, correspondingly. It was found that the films rotate in the direction of $\mathbf{E}_{ext} \times \mathbf{J}_{el}$, where this empirical rule was never violated in our experiments. This implies that the film rotation direction is independent of the choice of liquid film.

One simple explanation of the film rotation is the non-uniform distribution of the charges inside the liquid due to the external electric field (Grosu and Bologa 2010). In a conductive liquid (electrolyte), the current density, $\mathbf{J}$, is

Table 3 Non-rotational liquids

Name	μ (Debye)
1,4-Dioxane	0.45[a]
1-Bromo-4-fluorobenzene	0.42 ± 0.14[c]
1-Chlorodecane	1.9 ± 0.3[c]
1-Phenylhexane	0.20 ± 0.07[c]
cis-Decahydronaphthalene	0.006 ± 0.002[c]
Dodecane	∼0[b]
Mesitylene	0[b]
n-Dodecane	∼0[b]
5-Nonanol	1.7 ± 0.3[c]
Styrene	0.123[b]
tert-Butylcyclohexane	0.035 ± 0.012[c]

[a] http://macro.lsu.edu/howto/solvents/DipoleMoment.htm

[b] CRC Handbook of Chemistry and Physics, David R. Lide, ed., Internet Version 2005, http://www.hbcpnetbase.com, (CRC Press, Boca Raton, FL, 2005)

[c] Calculated by Gaussian98. The calculation error is about 20%

related both to the electric field, **E**, and charge diffusion as given by the Einstein–Nernst equation (Nelson 2003):

$$\mathbf{J} = \sigma\mathbf{E} - D\nabla\rho, \quad (1)$$

where D and σ are diffusion coefficient and conductivity of the liquid, respectively, and ρ is the charge density. On the other hand, the electric force density acting on the liquid is:

$$\mathbf{f} = \rho\mathbf{E}. \quad (2)$$

Since the applied torque, τ , is proportional to $\nabla \times \mathbf{f}$,

$$\tau \propto \nabla\rho \times \mathbf{E} + \rho\nabla \times \mathbf{E}. \quad (3)$$

In the steady state, $\nabla \times \mathbf{E} = 0$, therefore $\tau \propto \nabla\rho \times \mathbf{E}$. Substituting $\nabla\rho$ from Eq. 1, yields:

$$\tau \propto \mathbf{E} \times \mathbf{J}. \quad (4)$$

Hence, for a positive diffusion coefficient, the film should rotate in direction of $\mathbf{E} \times \mathbf{J}$, while the hydrodynamics controls velocity distribution on the film.

3.1.1 *Spatial angular velocity profile*

Figure 3 presents variational ensemble image velocimetry analysis of 30 double-frames corresponded to a Benzonitrile film, in a circular frame, rotating in an external electric field of magnitude 250 kv/m. The angular velocity radial profile, obtained as a function of the distance from the vortex, was found to decrease in an almost monotonic manner.

3.1.2 *The choice of liquid*

Measurements performed on different rotational liquids revealed that the angular velocity radial profile, in addition

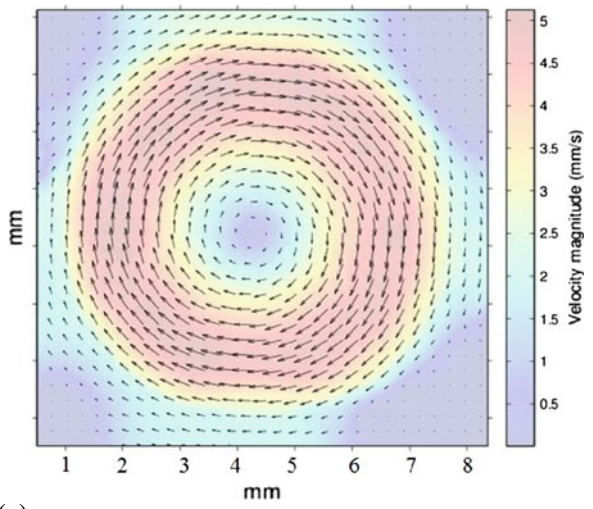

(a) Single-pixel resolution velocity field of the rotating film. The colormap is associated with velocity magnitude and the vectors represent the sub-sampled field.

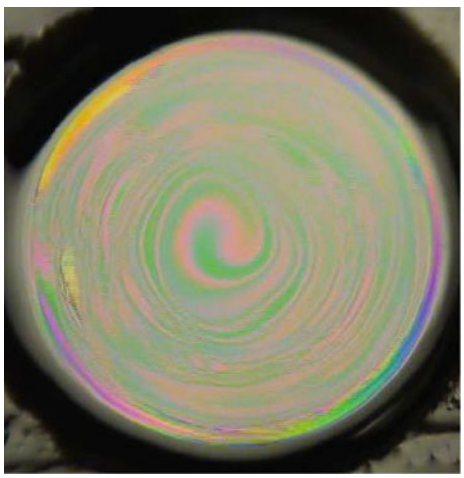

(b) A sample frame with radius of 3.5*mm* used in the image analysis.

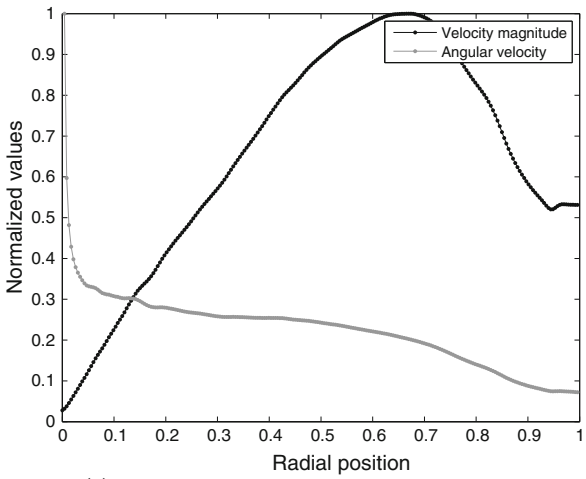

(c) The velocity and angular velocity normalized to the maximum value ($5mm/s$ and $2.5(1/s)$ respectively), and the radius normalized to $3.5mm$. The angular velocity decreases almost monotonically as a function of the distance to the vortex.

Fig. 3 Variational image velocimetry analysis of a rotating Benzonitrile film

to the applied electric field and electric voltage, depends on the choice of liquid. As an example, we applied image velocimetry on 1-Bromo-3-fluorobenzene and 2,5-Hexadione films for different electric field and voltage values, while $EV = \text{cte}$.

Figure 4 shows the obtained velocity fields for 1-Bromo-3-fluorobenzene, illustrating the threshold of rotation about $V = 140$ V and $E = 30$ kV/m. This also demonstrates how increasing the electric field and decreasing the electric voltage continuously changes the pattern of the rotation. Further increasing the electric field up to 210 kV/m and decreasing the electric voltage below 20 V impedes the rotation at the central region of the film.

On the other hand, as depicted in Fig. 5, similar measurements on 2,5-Hexadione showed that the rotation velocity pattern changes only slightly under the $EV = \text{cte}$ criterion.

3.1.3 Effect of V_{el}

Keeping the external electric field at a constant value, the angular velocity about the center of rotation was measured for different values of electrode voltage. Figure 6 shows the result for two rotational liquids, confirming that the films rotate faster when stronger electrode voltages are applied. In these experiments, the angular velocity was of the order of 10 Rad/s. This fast rotation creates radially homogeneous regions about the rotation center causing image velocimetry to be impossible. As a work around, the film was visualized using tracer particles; however, the displacements were too large to be reliably detected by image velocimetry. Due to this problem, the tracer particles were tracked manually.

3.1.4 Rotation threshold of rotational liquids

The studies on soap water films in Amjadi et al. (2009) reports that the rotation external electric field threshold, E_T, depends on the inverse of the applied electrode voltage magnitude V_{el}. Generalizing this rule to all rotational liquids, the E_T of each liquid was measured while V_{el} was set to the constant value of 25 V. As shown in Table 2, the resulting E_T values for the investigated rotational liquids are laid in the range of 51 to 228.5 kV/m.

The electric currents passing through the rotating films at the specified V_{el} are also presented in this table. Once the film rotation starts, the film thickness profile varies spatially, leading to a change of the film resistance. Due to this, the reported currents were measured just before the rotation started.

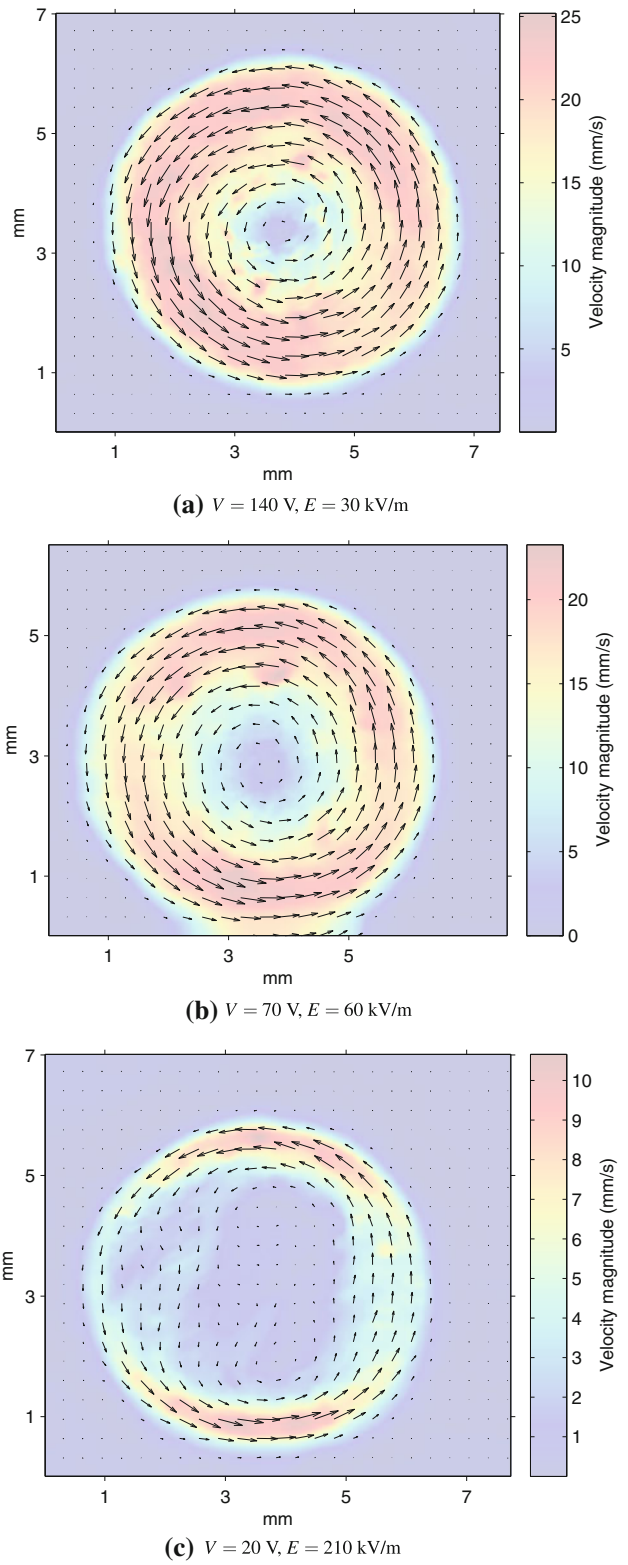

Fig. 4 Velocity field of a 1-Bromo-3-fluorobenzene film under different electric field and electrode voltage values, while $EV = \text{cte}$. The radius of frame is 3.5 mm

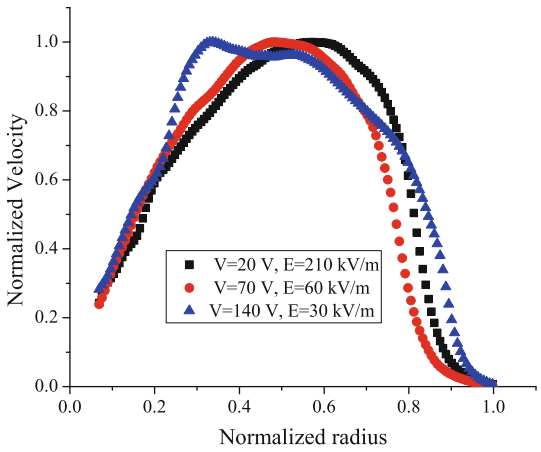

Fig. 5 Radial velocity profile of a 2,5-Hexadione film versus radius(normalized to 2.5 mm) under different electric field and electrode voltage values, where EV = cte. The velocities normalized to 19 mm/s (*square*), 20 mm/s (*circle*) and 31 mm/s (*triangle*)

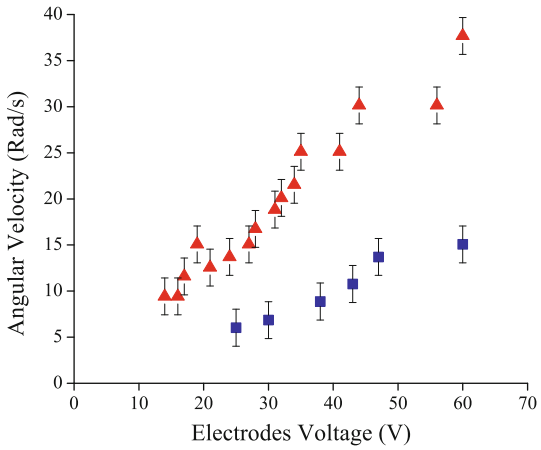

Fig. 6 The angular velocity increases with the applied electric voltage. Here, the angular velocities at the center and in a constant external electric field (E_{ext} = 240 kv/m) are presented for two liquids Benzonitrile (*triangles*) and 1-Methyl 2-pyrrolidone (*squares*). The other liquids (not presented here) show a similar trend

3.2 Correlation between liquid properties and film rotation threshold

Some properties of the studied rotational liquids (possibly relevant to the physics of the observed EHD effect) are given in Table 2. Of these properties, while density (ρ), viscosity (η), and critical force (η^2/ρ) may be relevant to hydrodynamics of the problem; the others, namely, dielectric constant (ε), conductivity (or films electric current I), molecular electric dipole moment (μ), and molar mass (M), may contribute to the electric force at macroscopic or microscopic scales.

Table 4 shows a quantitative measure of the relationship between E_T and the above-mentioned properties of the liquids, by presenting the calculated correlation coefficients and their measure of significance (p-value). Surprisingly, no significant correlation is observed between E_T and any of the liquid properties. Looking at the numbers, one may realize that the strongest correlation is associated with viscosity; however, this is not also significant enough. Moreover, in comparison with some of the properties that vary strongly and span a few orders of magnitude, the measured external electric field thresholds are laid within a very narrow window.

4 Discussion

The dominant deriving force in classical EHD theory comes from interactions between electric fields and charge/ion densities (Shiryaeva et al. 2009). Since the liquids conductivity depends on ion concentration and its mobility, it would be reasonable to expect a relationship between the electric current, I, passing through the film and the external electric field threshold, $\mathbf{E}_T$. Nonetheless, our experiments show that there is no such correlation between $\mathbf{E}_T$ and I exist, but it is also, among the very poor correlations

Table 4 Correlation between properties of the studied liquids and the rotation threshold of their films

Quantity/liquid category	Correlation				*P*-value			
	Rotating	Aromatic	Non-aromatic	Protic	Rotating	Aromatic	Non-aromatic	Protic
Critical force $\left(\frac{\eta^2}{\rho}\right)$	0.13	0.64	0.07	0.10	0.47	0.01	0.80	0.79
Density (ρ)	−0.08	0.05	0.07	0.43	0.65	0.81	0.80	0.28
Dielectric constant (ε)	0.19	0.12	0.04	0.09	0.37	0.66	0.89	0.80
Dipole moment (μ)	0.17	0.25	0.10	0.01	0.36	0.30	0.74	0.97
Electric current (I)[a]	0.06	0.12	−0.07	−0.03	0.72	0.59	0.82	0.93
Molar mass (M)	0.12	0.40	0.31	0.45	0.53	0.09	0.32	0.26
Viscosity (η)	0.21	0.62	0.01	0.13	0.25	0.01	0.98	0.74

The non-Newtonian liquid, Diiodomethane, is excluded

[a] The electric currents is not a liquid property, but it highly related to the electrical conductivity which is the liquid property

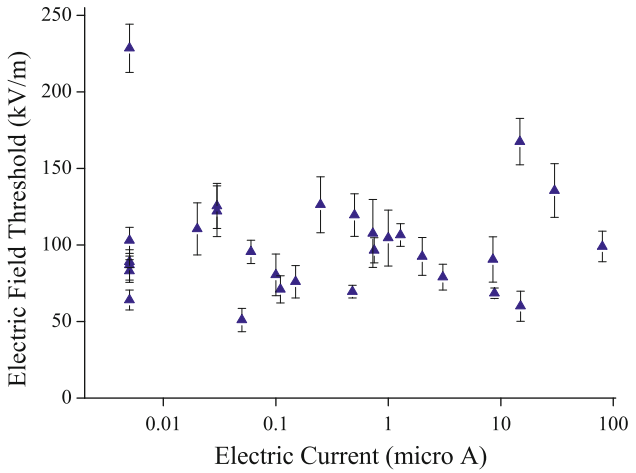

Fig. 7 The electric field threshold seems independent of the current passing through the films. While the electrical conductivity spans 4 orders of magnitude, the electric field thresholds do not vary significantly

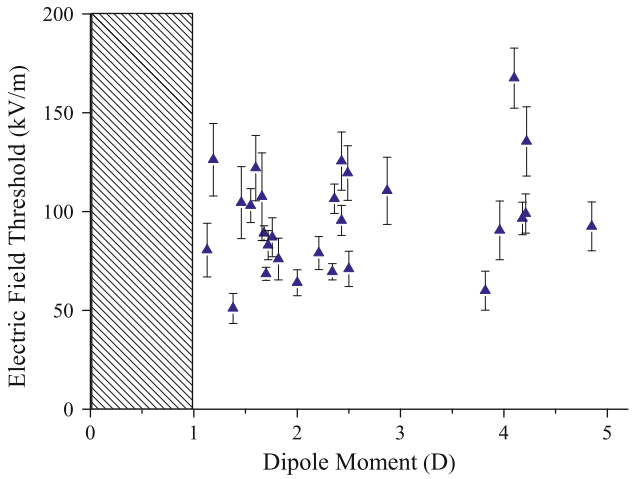

Fig. 8 Electric field threshold vs. molecular dipole moment of the rotating liquids. While all of the rotating liquids in our experiments have a molecular dipole moment of above 1 Debye, no remarkable correlation between the thresholds and dipole moments seems to exist

listed in Table 4, the electric current has the weakest one. Moreover, Table 3 shows that the electric currents passing through the liquid films (at a fixed voltage of 25 V) are very different and they actually vary by 4 orders of magnitude. It is interesting that even with such remarkable difference in the conductivity of rotating films, their electric field thresholds are nearly in the same order (Fig. 7). This insensitivity to the conductance has also been reported in the case of rotating soap water films by Amjadi et al. (2009), where the use of some additions (e.g. sodium chloride or sulfuric acid)–which is known to dramatically change the solution conductivity–was observed to have no effect on the rotation behavior.

As the center of the film rotates faster than the surrounding area which is revealed by the image velocimetry, it guides us to get the conclusion that a mechanism beyond charge electrophoresis is in work here (Amjadi et al. 2009).

Although in the list of the rotational liquids we have both good conducting liquids and poor conductors (with a current less than the sensitivity of our measuring device, i.e., 0.01 μA), all non-rotational liquids listed in Table 3 are poor conductors. In fact, we were not able to find any non-rotational liquids with good conductivity. Thus, we cannot completely wipe out the relevance of charge conductivity to the problem.

One clue which may help us to understand the physics of the problem is the common features between the rotational and non-rotational liquids, as well as the general differences between the two classes. However, as may be seen by comparing Tables 2 and 3, the non-rotational liquids are not very different from the rotational ones in most of their properties. As an interesting demonstration, we have tried three isomers of C_6H_4BrF. Two of these isomers, 1-Bromo-2-fluorobenzene and 1-Bromo-3-fluorobenzene, were classified as rotational liquids while the third one, 1-Bromo-4-fluorobenzene was observed to have a non-rotational film. Most of the physical and chemical properties of these isomers, if not exactly the same, are very close to each other, except two parameters: (a) electric conductivity and (b) molecular electrical dipole. As mentioned, all of the non-rotational liquids were found to be poor conductors. In addition, as depicted in Fig. 8, another common feature of the rotational liquids is that they consist of polar molecules with dipole moment above 1 Debye. Accordingly, the following one-way statement may be deduced: *For a rotating liquid film, it is a necessity to be polar, but this condition is not enough. By other means, all the rotating films are polar, but there are polar liquids such as 1-Chlorodecane and 5-Nonanol which do not rotate*.

5 Conclusion

Our experiments emphasize that the characteristics of the rotation for all of the rotational liquid films are similar to each other. That is, the direction of the rotation obeys the same rule. Moreover, the rotation speed is higher in stronger electric voltages.

The measurements also indicate that only polar liquids may produce rotating films and that all non-rotational liquids are insulator. Our measurements show that the best correlation between the threshold electric field and other discussed parameters is corresponded to the viscosity of the liquids with a value of 0.21, while its p-value of 0.25 is insignificant (Schervish 1996). Classifying all the rotating liquids to aromatic, non-aromatic, and protic shows that the

correlations are structure dependent. For example, we observed a significant correlation for both viscosity and critical force with a p-value of 0.01. Consequently, in order to have a liquid film motor, the dipole moment has a vital role; however, it is not the only effective parameter and for understanding the dominant mechanism we need to consider the contribution of molecular structure as well as other physical properties.

Acknowledgments We would like to thank Nima Hamedani Radja, Behrouz Eslami, and Kourosh Malek for their useful comments and discussions; Ahmad Ramazani S. A. and Meysam Nourani from Rheology Laboratory of Chemical Engineering Department for measuring the viscosity, Hadi Nazari, Reza Mozaffari, Ali Mahdavi, Ammar Nejati, Farzad Saidi, Mehrnush Naderi, Mojtaba Amini, Behzad Khalili, Majid Mosayebi, and Farid Taherkhani for their technical helps and comments; and the Center of Excellence in Complex Systems and Condensed Matter (CSCM) and Sharif Applied Physics Center for their support of this project.

References

Adrian R, Wildes RP, Amabile MJ, marie Lanzillotto A, shyng Leu T (1991) Particle imaging techniques for experimental fluid mechanics. In: In Proc Conf Comp Vision Pattern Rec, pp 969–975

Amjadi A, Shirsavar R, Radja NH, Ejtehadi MR (2009) A liquid film motor. Microfluidics and Nanofluidics 6 (5):711–715

Chandrasekhar S (1992) Liquid crystals. Cambridge University press, New York

Chiragwandi ZG, Nur O, Willander M, Panas I (2005) Appl Phys Lett 87:153,109

Chomaz JM, Cathalau B (1990) Soap films as two-dimentional classical fluids. Phys Rev A 41:2243

Couder Y, Chomaz JM, Rabaud M (1989) On the hydrodynamics of soap films. Physica D 37:384–405

Daya ZA, Morris SW, deBruyn JR (1997) Phys Rev E 55:2682

de Gennes PG, Prost J (1995) The physics of liquid crystals. Oxford University Press, New York

Deen DW, Delnoij E, Westerweel J, Deen NG, Kuipers JAM, Swaaij WPMV (1999) Ensemble correlation piv applied to bubble plumes rising in a bubble column

Faetti S, Fronzoni L, Rolla PA (1983a) J Chem Phys 79:1427

Faetti S, Fronzoni L, Rolla PA (1983b) J Chem Phys 79:5054

Green NG, Ramos A, Gonzalez A, Morgan H, Castellanos A (2000) Fluid flow induced by nonuniform ac electric fields in electrolytes on microelectrodes. I. experimental measurements. Physical Review E 61(4):4012

Grosu FP, Bologa MK (2010) Electroconvective rotation of a dielectric liquid in external electric fields. Surf Eng Appl Electrochem 46 (1):43–47

Horn BKP, Schunck BG (1981) Determining optical flow. Artif Intell 17:185–203

Huang MJ, Wen CY, Lee IC, Tsai CH (2004) Air-damping effects on developing velocity profiles in flowing soap films. Phys Fluid 16:3975

Isenberg C (1992) The science of soap films and soap bubbles. New York

Morris SW, Debbuyn JR, May AD (1990) Phys Rev Lett 65:2378

Nelson P (2003) Biological physics: energy, information, life. W. H. Freeman, New York

Rivera M, Wu XL (2000) External dissipation in driven two-dimensional turbulence. Phys Rev Lett 85:976

Ruhnau P, Kohlberger T, Nobach H, Schnörr C (2005) Variational optical flow estimation for particle image velocimetry. Exp Fluids 38:21–32

Rutgers MA, Wu XL, Daniel WB (2001) Fluid flow induced by nonuniform ac electric fields in electrolytes on microelectrodes. i. experimental measurements. Rev Sci Instrum 72:3025

Saville DA (1997) Electrohydrodynamics: the taylor-melcher leaky dielectric model. Annu Rev Fluid Mech 29:27–64

Schervish MJ (1996) P value: what they are and what they are not? Am Statistican 50(3):203–206

Shiryaeva EV, Vladimirov VA, Zhukov MY (2009) Theory of rotating electrohydrodynamic flows in a liquid film. Phys Rev E 80(4):041,603

Sonin AA (1998) Freely suspended liquid crystalline films. Wiley, New York

Westerweel J (1993) Digital particle image velocimetry—theory and application. PhD thesis, Delft University of Technology, Delft